Supporting Information

Liquid-Phase Exfoliation of Graphite into Single- and Few-Layer Graphene with α-Functionalized Alkanes

Sébastien Haar,[†] Matteo Bruna,[§] Jian Xiang Lian,[‡] Flavia Tomarchio[§], Yoann Olivier,[‡] Raffaello Mazzaro,[||,Δ] Vittorio Morandi,[||] Joseph Moran,[†] Andrea C. Ferrari,[§] David Beljonne,[‡] Artur Ciesielski[†] and Paolo Samorì[†]

† Institut de Science et d'Ingeńierie Supramolećulaires (ISIS) and International Center for Frontier Research in Chemistry (icFRC), Université de Strasbourg and Centre National de la Recherche Scientifique (CNRS), 8 alleé Gaspard Monge, 67000 Strasbourg, France.

§ Cambridge Graphene Centre, University of Cambridge, 9 JJ Thomson Avenue, Cambridge, CB3 0FA, UK

‡ Université de Mons, Place du Parc, 20, 7000 Mons, Belgium.

|| Consiglio Nazionale delle Ricerche (CNR), Istituto per la Microelettronica e i Microsistemi (IMM) Sede di Bologna, Via Gobetti 101, 40129 Bologna, Italy

Δ Dipartimento di Chimica "G. Ciamician", Università di Bologna, Via Selmi 2, 40126 Bologna, Italy.

Table of content

S1. Materials and methods

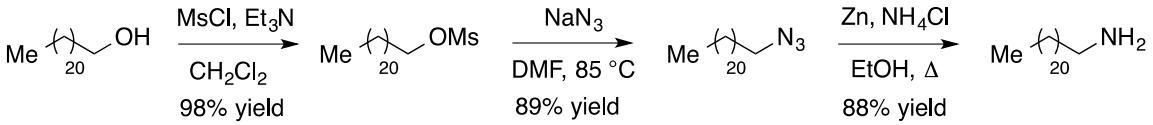

Docosan-1-amine. The compound is prepared with 77% yield over three steps from 1-docosanol according to a modification of the procedure of Ref.[1] 1-Docosanol (8.17 g, 25.0 mmol, 1 equiv) and Et_3N (5.82 g, 8.02 mL, 57.5 mmol, 2.3 equiv) are dissolved in CH_2Cl_2 under magnetic stirring and the solution is cooled to 0 °C with the use of an ice bath. Mesyl chloride (4.6 g, 3.1 mL, 40 mmol, 1.6 equiv) is added dropwise by syringe over 5 min. The ice bath is then removed and the reaction stirred for 3 h while being allowed to warm to ambient temperature. The resulting yellow solution is washed successively with water (25 mL), 2 M HCl (25 mL) and water (25 mL). The organic phase is dried with $MgSO_4$ and concentrated under reduced pressure to give crude docosyl mesylate as a white-yellow solid (9.89 g, 98%) that is used without further purification. In a 500 mL round bottom flask equipped with a reflux condenser, docosyl mesylate (9.89 g, 24.4 mmol, 1 equiv) is dissolved in DMF (163 mL), followed by the addition of NaN_3 (3.97 g, 61.0 mmol, 2.5 equiv). The mixture is stirred for 30 min at ambient temperature and then heated to 85 °C using an oil bath for 4 h. TLC (10% EtOAc:Pentane) indicated complete consumption of the mesylate. The reaction is then cooled to ambient temperature and then diluted with petroleum ether (300 mL) and water (30 mL). The organic layer is separated and then washed with saturated $NaHCO_3$ (30 mL) and brine (30 mL). The organic layer is dried over Na_2SO_4 and concentrated under reduced pressure to give a crude solid (8.06 g), purified by silica gel chromatography (Pet. Ether) to give 1-azidodocosane as a sticky white solid (7.65 g, 89%). The reduction of the azide to the amine is carried out according to a modification of the procedure of Ref.[2] Ethanol (53 mL) and deionized water (22 mL) are added to a mixture of 1-azidodocosane (7.0 g, 19.9 mmol, 1 equiv) and ammonium chloride (2.45 g, 45.8 mmol, 2.3 equiv) in a 250 mL round bottom flask equipped with a reflux condenser. The solids do not completely dissolve. Zinc powder (1.69 g, 25.9 mmol, 1.3 equiv) is then added and the heterogeneous mixture heated to reflux for 10 minutes, at which time TLC (Petroleum

ether 100%) indicates that all starting materials are consumed. The reaction mixture is cooled to ambient temperature and then petroleum ether (200 mL) and aqueous ammonia (10 mL) are added. The mixture is filtered through celite, washed with brine, dried over Na_2SO_4 and concentrated under reduced pressure to give 6.30 g of a sticky off-white solid. Recrystallization from EtOAc yields the title product as a white solid (5.71 g, 88%). ^{1}H NMR data is consistent with that described previously in the literature.[1]

In order to obtain dispersions, graphite flakes are sonicated for 6 h at 50 ± 2°C (600 W) in (9.71 mL) NMP, keeping the graphite weight percent constant, i.e. 1 wt%. Different masses of dispersing-stabilizing agents are used depending on s.a. %, see table S1.

Table S1. Masses of organic molecules used in LPE process.

	Mass for each surface area (in mg)					
	2.5 %	5 %	7.5 %	10 %	15 %	20 %
Graphene exfoliated with ***Amine***	2.375 mg	4.75 mg	7.15 mg	9 mg	14.25 mg	19 mg
Graphene exfoliated with ***Alcohol***	2.25 mg	2.25 mg	6.75 mg	8 mg	13.5 mg	18 mg
Graphene exfoliated with ***Carboxylic acid***	2.5 mg	5 mg	7.5 mg	10 mg	15 mg	20 mg
Graphene exfoliated with ***Alkane***	2.25 mg	2.25 mg	6.75 mg	8 mg	13.5 mg	18 mg

S2. UV-Vis-IR spectroscopy

All dispersions are also characterized by UV–vis–IR absorption spectroscopy. Each is diluted a number of times and the absorption recorded. The absorbance (660 nm) divided by cell length is plotted versus concentration. A Lambert – Beer behavior is observed for all samples.

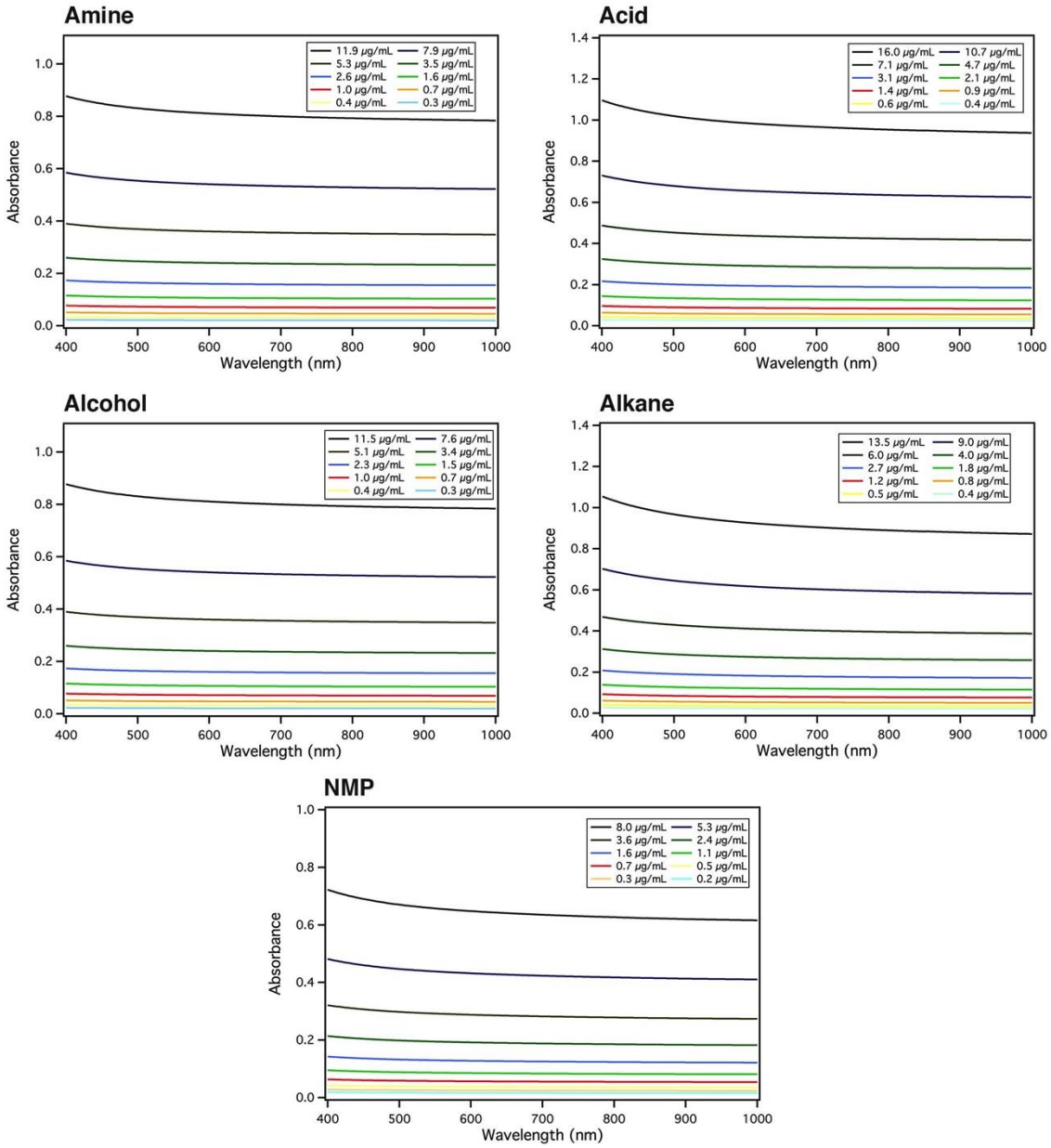

Figure S1. UV–Vis spectra of dispersions in NMP in the presence/absence of dispersing-stabilizing agents at different concentrations for 20 s.a. %.

S3. Molecular Dynamics

3.1 Atomistic representations of the SAM architectures

From the lattice parameters reported in Table 1 of the main text, SAMs are prepared using a cluster approach. As the unit cells of the dispersion-stabilizing molecules do not match the unit cell of graphene, it is not possible to work in periodic boundary conditions. In order to reduce the impact of edge effects on the estimation of interaction energies large SAMs are thus built, based on a 9×5 supercell architectures (i.e., 45 molecules) for docosane and docosan-1-amine, and 6x5 supercell for docosanoic acid molecules (i.e., 60 molecules). The underlying graphene consists of 5680 carbon atoms in a rectangular box with dimension of ~ 8.5 × 17.5 nm^2 (Figure S3).

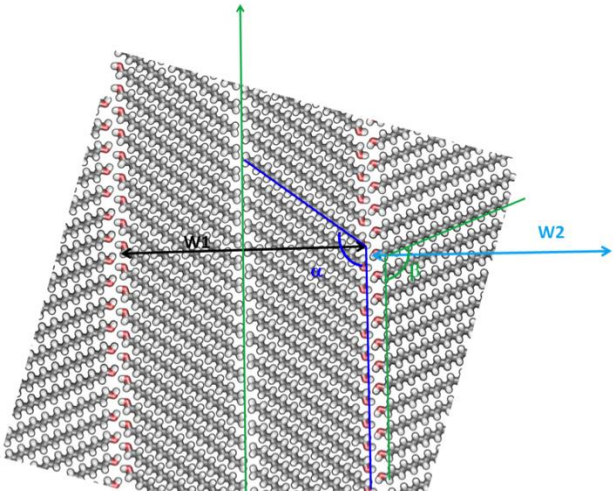

Figure S2. Geometrical parameters describing the docosanol SAM: *W1* and *W2* are the widths of the stacks and α and β, the tilt angles of the docosanol molecules with respect to the stacking direction

In the case of the docosanol molecule, no clear unit cell can be deduced because of the different orientations of the molecules in different lamellae (Figure 1g,h). Therefore, we define complementary parameters for the relative orientations of the molecules within the SAM: *W1* and *W2*, i.e. the widths of the two stacks in Figure S2 and α and β the tilt angles of the docosanol molecules with respect to the stacking direction. Experimentally, *W1* and *W2* are ~4.78 ± 0.2 nm and 5.21 ± 0.3 nm while α = 128 ± 1 and β =111 ± 1 degrees, respectively.

For the docosanol, two model systems made of two parallel stacking are built, (i) one where the functional groups are facing each other within the parallel stack (head-head) and (ii) another one where the methyls are facing each other to test the relative stability of these two orientations. It is found that system (i) is more stable than (ii). The tilts (change of chain axis direction, Figure 1) preferentially occur at the methyl-methyl junction. On that basis, a 'trial' system consisting of 45 docosanol molecules has been placed on a graphene surface (~15×10 nm²) containing 5600 carbon atoms, as depicted in Figure S4 and the structure has been optimized. Finally, taking into account the similarities of the lattice parameters between docosane and docosan-1-amine, the SAM of the amine derivative (not shown) has been prepared based on the docosane structure.

The systems are optimized with the Accelrys Materials Studio software package using the Dreiding force-field in vacuum.[3] Then, we proceed with an optimization (minimization and equilibration at 300 K with the Gromacs 6.2 software[4]) of the SAM-SLG systems performed with NMP solvent.

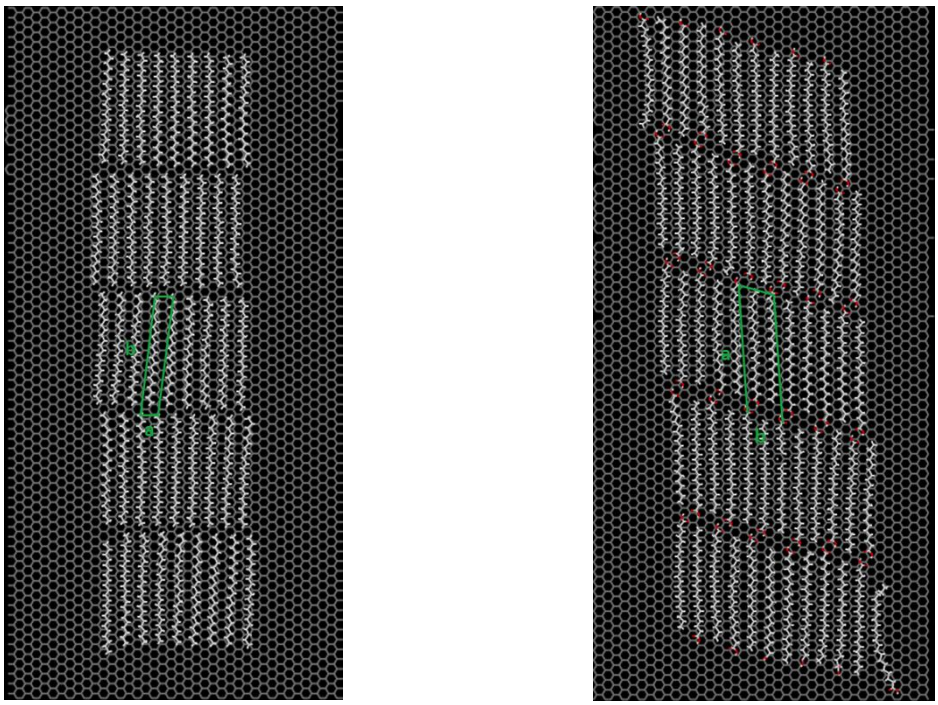

(a) docosane SAM **(b) docosanoic acid SAM**

Figure S3. Structure of the SAM after NVT equilibration at 300 K. (a) Docosane SAM: $\boldsymbol{a}$ = 0.45 ± 0.03 nm, $\boldsymbol{b}$ = 3.01 ± 0.03 nm, and $\boldsymbol{\alpha}$ = (86.05 ± 1.7)°. (b) Docosanoic SAM: $\boldsymbol{a}$ = 3.22 ± 0.11 nm, $\boldsymbol{b}$ = 0.92 ± 0.04 nm, and $\boldsymbol{\alpha}$ = (70.43 ± 3.9)°. The unit cells (shown in green) are estimated from the center of the SAM

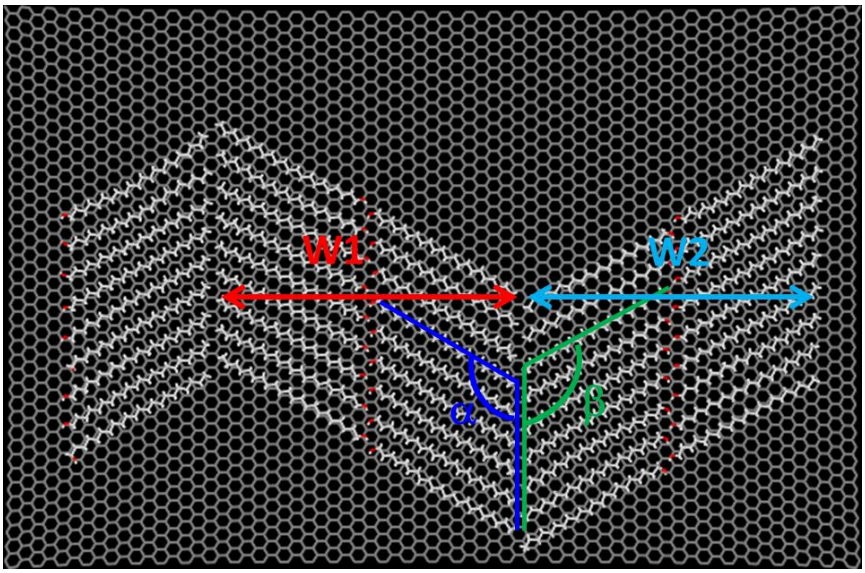

Figure S4. Structure of the **docosanol** SAM after NVT equilibration at 300 K. The parameters are estimated from the center of the SAM: *W1* = 5.27±0.1 nm, *W2* = 5.23±0.1 nm, α = (119.64 ± 1)°, and β = (120.25 ± 1.7)°

The SAM for docosane and docosanoic acid molecules obtained from the simulations present the same features as those observed in the STM images (Figure 1 of the main text). The methyl groups of each docosane molecule are slightly shifted in order to maximize the interactions with the molecules in adjacent lamellae. The lamella axis is almost perpendicular to the chain axis. A rough estimate of the unit cell is made by taking into account only the 15 molecules closer to the center of the SAM (i.e., two docosane molecules at each edge, as well as the most two external lamellae were neglected). The lattice parameters are ***a*** = 0.45 ± 0.03 nm, ***b*** = 3.01 ± 0.03 nm, and ***α*** = 86.05 ± 1.7 degree for the docosane and ***a*** = 3.22 ± 0.11 nm, ***b*** = 0.92 ± 0.04 nm, and ***α*** = 70.43 ± 3.9 degrees for the docosanoic in a rather good agreement with the experimental values (Table 1). For the docosanol SAM (Figure 2.17), the widths of the two stacks are estimated to be *W1* = 5.27±0.1 nm and *W2* = 5.23±0.1 nm. The angles, calculated with respect to the lamella axis, are: α = (119.64 ± 1) ° and β = (120.25 ± 1.7) °. This indicates that the docosanol SAM is almost symmetric, unlike the experiments (Table 1). A possible explanation of this deviation might be that the cluster is too small and the docosanol molecules easily move over time (small reorganization of the SAM). Moreover, the estimation of the lattice parameters is less trivial in the case of docosanol molecule. Nevertheless, the cohesion of the SAM is preserved at room temperature thanks to the favorable CH_2-CH_2

interactions and H-bonds, which stabilize the SAM. In Figures S5 and S6, we report snapshots (top view and perspective view, respectively) of the MD simulations taken at 4 ns after (the simulation time was 5 ns).

3.2 Force field parameterization

We use the optimized potentials for liquid simulations – all atoms (OPLS-AA) force field since it has been proven to properly describe the aliphatic chains in liquid media[5-7] and studied with various polar solvent, including NMP.[8-10] The Lennard Jones (LJ) coefficients for atoms of different kinds are obtained as a geometric mean value of the parameters of two corresponding particles:

$$\epsilon_{ij} = \sqrt{\epsilon_{ii}.\epsilon_{jj}} \qquad \sigma_{ij} = \sqrt{\sigma_{ii}.\sigma_{jj}}$$

where the subscripts *i* and *j* indicate the particle types.

Our MD simulations verify that such a parameterization leads to a density in good agreement with experiments (1.028 g/cm³). Regarding the electrostatic interactions, no partial charge is attributed to the graphene surface, while the partial charges of the alkyl molecules are assigned according to the OPLS-AA force field.

3.3 Molecular dynamics simulation details

During the preparation of the systems prior to the MD production simulations, the leap-frog integrator is used with a time step of 2×10^{-3} ps.[11] The LJ potential is treated by the cut-off method,[11] while the Particle Mesh Ewald method[12] is used for the treatment of the long-range electrostatic interactions with 0.12 nm spacing for the mesh in the real space. The non-bonded interactions account for a cut-off radius of 1.3 nm, and the neighbor list is updated each 10th integration step, using the grid method.[13] The lengths of bonds involving hydrogen atoms are constrained to the force field equilibrium to speed up calculations.

The systems are prepared such as we have solvated the MOL-SLG complex using 1134 NMP molecules in order to set up the density according to the experimental NMP density. The systems are minimized according to the steepest descent algorithm

implemented in GROMACS to a 10 J/nm force tolerance, and then gradually heated in the NVT ensemble[14] (Berendsen thermostat, coupling constant=1ps), likewise, a 10-ps NVT equilibration simulation at 100, 200 and 300 K. From the output configuration of the heating process, we simulate for 200 ps in the NPT ensemble (Berendsen thermostat and Berendsen barostat, coupling constant=1ps)[10] at 300K for an external pressure of 1 bar to equilibrate the density of the systems. Finally, 300-ps equilibration and 1-ns production MD simulations are carried out in the NVT ensemble (Berendsen and Nosé-Hoover thermostats, respectively), while using a 1.3-nm cut-off for the treatment of the long-range electrostatic interactions.

3.4 Estimating the stability of the molecules on graphene

a. Interaction energy of one stabilizing-agent molecule within the SAM

Along molecule-surface, solvent-surface and molecule-solvent interactions, the supramolecular organization of the dispersion-stabilizing molecules on graphene results from a combination of stabilizing van der Waals interactions between alkyl chains and the surface, intermolecular interactions within a given lamella, and hydrogen bonds between the head groups belonging to adjacent lamellae. In order to quantify all these interactions and rationalize the exfoliation yields we perform MD simulations using the GROMACS 6.2 MD software. SAMs of the different agents in Scheme 1 are modeled as defect-free 2d lattices interacting with the solvent and the substrate underneath. Then, the internal energy of the central monomer in the 2d lattice was determined as:

$$E_{int}^{SAM} = E_c^{SAM} + E_{mol-sam} + E_{mol-slg} + E_{mol-sol} \quad \text{(S1)}$$

where $E_{mol\text{-}sam}$, $E_{mol\text{-}slg}$, and $E_{mol\text{-}sol}$ are the interaction energies between the molecule with the monolayer, graphene surface and solvent, respectively. E_c^{SAM} is the valence term, which includes bonds, angles, dihedrals, and intramolecular interactions within the monomer in the 2d lattice. All terms in Equation (S1) are evaluated using the *g_energy* program of GROMACS, where *mol* refers to the central molecule of the SAMs used as reference for the calculations (see Figures S3, S4). The same equation is used to calculate the internal energy of the monomer in the solvent phase (SOL superscript instead of SAM). Interaction energy per unit area is calculated by dividing E_{int} in Equation (S1) by the estimated unit cell area of the dispersion-stabilizing agent (see Table S2).

The adsorption of the four molecules in Scheme 1 on graphene is determined from the analysis of the thermodynamic stability of their SAMs. The binding affinity of a monomer for graphene depends on the interplay between the energy gain due to its adsorption and interaction with the substrate and other molecules, and the entropy cost of its confinement in the monolayer.

b. Free energy of adsorption at the graphene surface

To evaluate the entropic cost of confining the monomer from solvent-phase into a monolayer, the major contributions to the overall entropy loss are assumed to be the

translational entropy and rotational entropy. They correspond to the reversible work of confining the molecules diffusing in NMP solvent to a 2d lattice on graphene. Assuming the monomers are not interacting with themselves, and zero translational and rotational entropy in the SAM, the entropy loss can be evaluated analytically using the Sackur-Tetrode formula.[15] The translational entropy is expressed as:

$$S_{tr} = R\left[\frac{5}{2} + \ln\left(\frac{2\pi m k_B T}{h^2}\right)^{\frac{3}{2}} - lnC\right] \quad \text{(S2)}$$

with m the mass of the molecule, T the absolute temperature, k_B the Boltzmann constant, h the Planck constant, and C the concentration of monomers in the solvent-phase. The rotational entropy contribution is expressed as:

$$S_{rot} = R\left[\frac{3}{2} + \ln\left(\frac{8\pi^2 m k_B T}{h^2}\right)^{\frac{3}{2}} + ln\frac{\sqrt{\pi}}{\sigma} + \frac{1}{2}\ln(I_A I_B I_C)\right] \quad \text{(S3)}$$

with I_A, I_B, and I_C the three principal moments of inertia of the monomer, and σ is the symmetry number of the monomer.

Within the approximations inherent to the model, Equations (S1) – (S3) estimate the free energy change of the self-assembly formation $nX \rightarrow X_n$, with X the monomer in the solvent phase, X_n the monolayer on the substrate, and n the number of molecules required to cover the surface area A. From the unit cell parameters which can be obtained either by STM or molecular modeling, the stoichiometric coefficient of the self-assembly reaction is given by:

$$n = \frac{A}{A_{uc}} n_{uc} \quad \text{(S4)}$$

with A the surface area to be covered, A_{uc} the unit cell area of the 2d lattice, and n_{uc} the number of molecules in the unit cell. The energy gain upon formation of the SAM on graphene is:

$$\Delta E = n(\, E_{int}^{SAM} - \, E_{int}^{solvent}\,) \quad \text{(S5)}$$

where $E_{int}^{solvent}$ is the internal energy of a monomer in the solvent phase calculated with Equation (S1). And, the entropic cost of confinement is:

$$\Delta S = -n(S_{tr} + S_{rot}) \quad \text{(S6)}$$

Using the results of Equations (S5,6), the free energy of self-assembly formation per surface area A is given by:

$$\Delta F = \Delta E - T\Delta S \quad \text{(S7)}$$

which corresponds to the reversible work of confining n monomers from the solvent phase to a monolayer on graphene. Equation (S7) evaluates the ability of a monomer of forming a 2d lattice on graphene at a given experimental conditions (T, C, etc.), and can be used to predict the dispersion-stabilization efficiency of the molecule.

3.5 Results

a) SAMs of dispersion-stabilizing agents physisorbed on the graphene surface

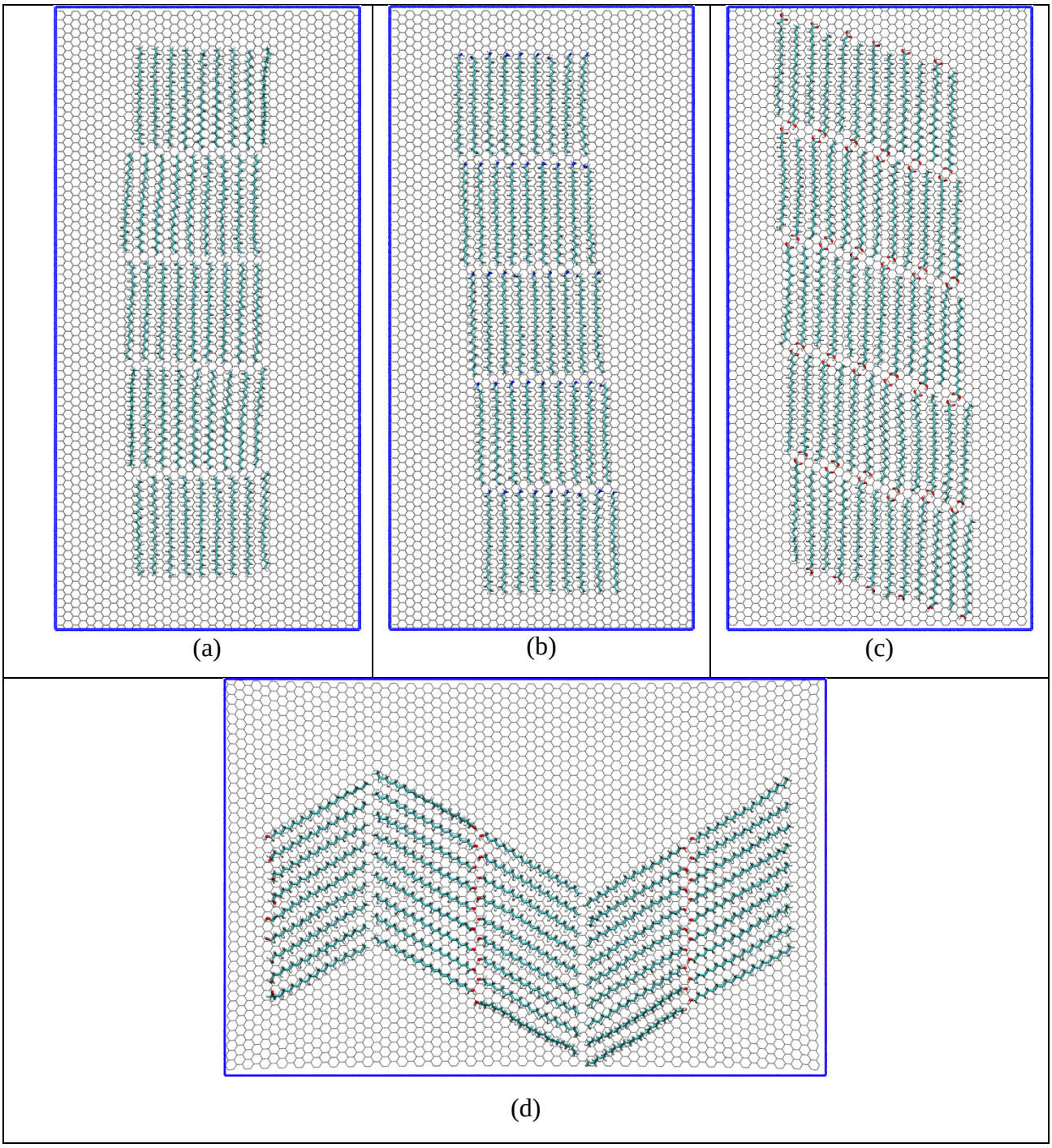

Figure S5. Snapshot (top view) after 4 ns of NVT equilibration at 300 K: a) docosane, b) docosan-1-amine, c) docosanoic acid, and d) docosanol.

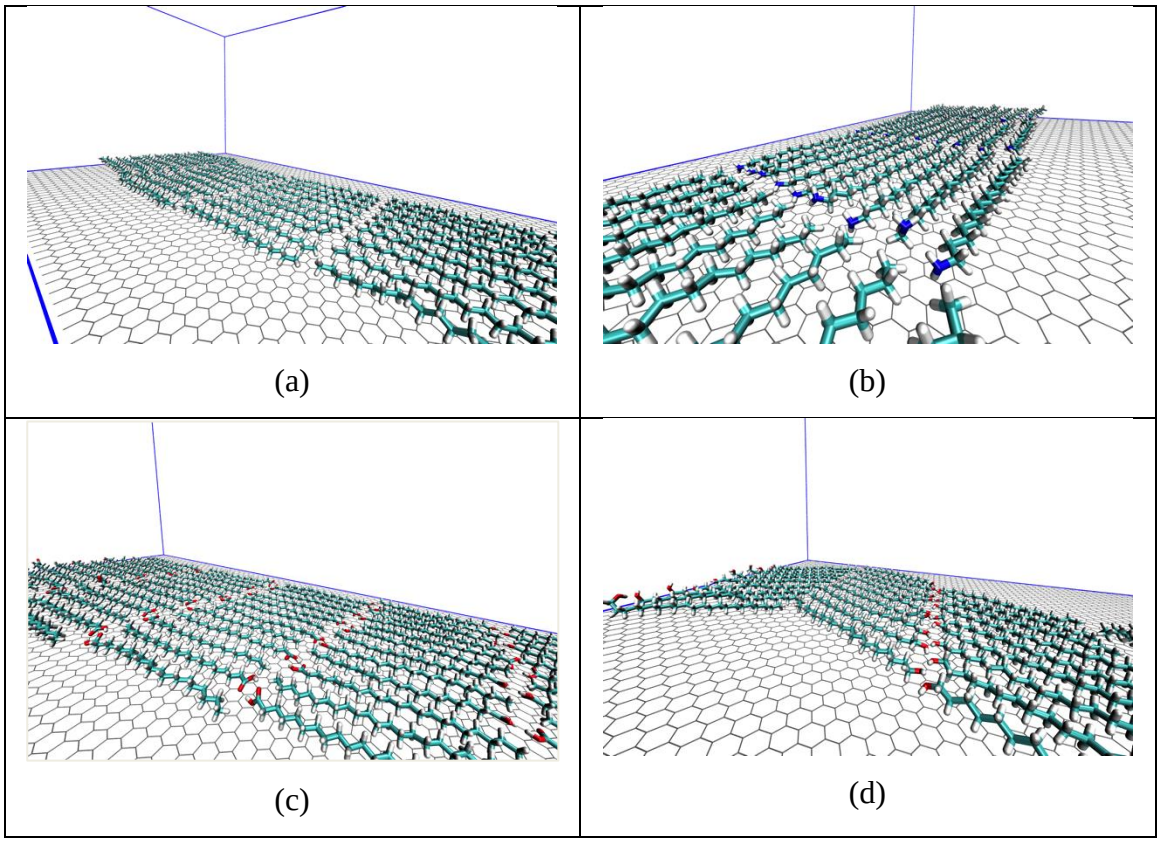

Figure S6. Snapshot (perspective view) of NVT equilibration at 300 K: a) docosane, b) docosan-1-amine, c) docosanoic acid, and d) docosanol.

b) Interaction energy of one stabilizing-agent molecule within the SAM

Table S2. Modeled energy, entropy and free energy for the self-assembly on graphene of alkyl chains functionalized with different functional groups in NMP. A 1 nm² area and a solute concentration of 2 mM are used. The stoichiometric coefficients of the self-assembly reaction (n) described by Eq. S4 and the number of molecules per unit cell, n_{uc}, are given. The temperature is set to 300 K. All energies are given per molecule and expressed in kJ mol^{-1}. The symmetry number of the monomer is set to unity for all molecules, i.e. Cs symmetry. The experimental unit-cell area obtained from STM are used for all agents.

c)

	A_{uc}	n_{uc}	n	$T\,S_{trans}$	$T\,S_{rot}$	E_c^{SAM}	$E_{mol-sam}^{SAM}$	$E_{mol-slg}^{SAM}$	$E_{mol-sol}^{SAM}$	E_c^{SOL}	$E_{mol-sol}^{SOL}$	ΔE	$-T\,\Delta S$	ΔF
CH_3	1.2	1	0.83	62.0	47.4	178.7	-266.5	-164.8	-104.5	221	-265.4	-260.5	91.1	-169.4
OH	2.4	2	0.83	62.1	47.9	184.6	-278.5	-173.8	-105.6	221	-296.8	-247.7	91.7	-156.0
NH_2	1.2	1	0.83	62.1	47.8	178.1	-261.1	-170.9	-104.8	216	-291.9	-235.7	91.6	-144.1
COOH	2.8	2	0.71	62.3	48.3	105.9	-286.7	-175.7	-105.7	148.3	-318.5	-208.6	79.0	-129.6
COOH x2	2.8	1	0.36	64.9	55.4	165.7	-465	-347.7	-223.6	294.4	-634.7	-189.4	43.0	-146.4

Table S3. Decomposition of the total interaction energy per molecule of docosane, docosanol, docosan-1-amine, and docosanoic acid monomers in the center of the SAM with the SAM molecules, the graphene surface and the NMP solvent (cutoff radius of 1.3 nm). All energies are given per molecule and expressed in kJ mol^{-1}. LJ and Q denote vdW and Coulomb interactions, respectively.

	A_{mol}	$E_{MOL-SAM}^{Q}$	$E_{MOL-SAM}^{LJ}$	$E_{MOL-SAM}^{LJ+Q}$	$E_{MOL-SLG}^{LJ}$	$E_{MOL-NMP}^{Q}$	$E_{MOL-NMP}^{LJ}$	$E_{MOL-NMP}^{LJ+Q}$	E_{tot}
CH_3	1.2	0.8	-118.9	-118.1	-164.7	0.3	-99.6	-99.3	-382.1
OH	1.5	-55.9	-113.5	-169.4	-170.1	-0.9	-103.6	-103.6	-443.0
NH_2	1.4	-5.4	-121.3	-126.8	-171.7	-6.6	-102.6	-109.3	-407.7
COOH	1.3	-49.5	-116.5	-166.0	-173.6	-1.2	-107.0	-108.1	-447.7

*Areas (occupied by single molecules within the unit cell) are calculated from averaged distances between adjacent alkyl chains (excluding the monomers at the edges) in the optimized geometries of the SAM (see Figures S3 and S4, supporting information).

The binding affinity of a monomer for graphene depends on the interplay between the energy gain due to its adsorption and interaction with the substrate and other molecules,

and the entropy cost of its confinement in the monolayer. The Sackur-Tetrode equations allow us to estimate these contributions in the limit of the approximations (Equations S1-S3). The free energy of adsorption of the four agents proposed in Figure 1 (main text) are given in Table S3 in addition to (decomposition of) the change of internal energy and entropy cost. The results for a docosanoic acid dimer are also given.

References

1. Sugandhi, E. W.; Macri, R. V.; Williams, A. A.; Kite, B. L.; Slebodnick, C.; Falkinham, J. O.; Esker, A. R.; Gandour, R. D. Synthesis, Critical Micelle Concentrations, and Antimycobacterial Properties of Homologous, Dendritic Amphiphiles. Probing Intrinsic Activity and the "Cutoff" Effect. *J. Med. Chem.* **2007,** *50*, 1645-1650.
2. Lin, W. Q.; Zhang, X. M.; Ze, H.; Yi, J.; Gong, L. Z.; Mi, A. Q. Reduction of Azides to Amines or Amides with Zinc and Ammonium Chloride as Reducing Agent. *Synth. Commun.* **2002,** *32*, 3279-3284.
3. Mayo, S. L.; Olafson, B. D.; Goddard, W. A. Dreiding - a Generic Force-Field for Molecular Simulations. *J. Phys. Chem.* **1990,** *94*, 8897-8909.
4. Van der Spoel, D.; Lindahl, E.; Hess, B.; Groenhof, G.; Mark, A. E.; Berendsen, H. J. C. GROMACS: Fast, Flexible, and Free. *J. Comp. Chem.* **2005,** *26*, 1701-1718.
5. Jorgensen, W. L.; Maxwell, D. S.; TiradoRives, J. Development and Testing of the OPLS All-Atom Force Field on Conformational Energetics and Properties of Organic Liquids. *J. Am. Chem. Soc.* **1996,** *118*, 11225-11236.
6. Price, M. L. P.; Ostrovsky, D.; Jorgensen, W. L. Gas-Phase and Liquid-State Properties of Esters, Nitriles, and Nitro Compounds with the OPLS-AA Force Field. *J. Comput. Chem.* **2001,** *22*, 1340-1352.
7. Thomas, L. L.; Christakis, T. J.; Jorgensen, W. L. Conformation of Alkanes in the Gas Phase and Pure Liquids. *J. Phys. Chem. B* **2006,** *110*, 21198-21204.
8. Aparicio, S.; Alcalde, R.; Davila, M. J.; Garcia, B.; Leal, J. M. Measurements and Predictive Models for the N-methyl-2-pyrrolidone/water/Methanol System. *J. Phys. Chem. B* **2008,** *112*, 11361-11373.
9. Frolov, A. I.; Arif, R. N.; Kolar, M.; Romanova, A. O.; Fedorov, M. V.; Rozhin, A. G. Molecular Mechanisms of Salt Effects on Carbon Nanotube Dispersions in an Organic Solvent (N-methyl-2-pyrrolidone). *Chem. Sci.* **2012,** *3*, 541-548.
10. Shih, C. J.; Lin, S. C.; Strano, M. S.; Blankschtein, D. Understanding the Stabilization of Liquid-Phase-Exfoliated Graphene in Polar Solvents: Molecular Dynamics Simulations and Kinetic Theory of Colloid Aggregation. *J. Am. Chem. Soc.* **2010,** *132*, 14638-14648.
11. Berendsen, H. J. C.; van Gunsteren, W. F. In *Molecular Dynamics Simulation of Statistical Mechanical Systems*, Ciccotti, G.; Hoover, W., Eds. Soc. Italiana di Fisica, Bologna: North Holland; Amsterdam, 1986; p 43.
12. Essmann, U.; Perera, L.; Berkowitz, M. L.; Darden, T.; Lee, H.; Pedersen, L. G. A Smooth Particle Mesh Ewald Method. *J. Chem. Phys.* **1995,** *103*, 8577-8593.
13. Lindahl, E.; Hess, B.; van der Spoel, D. GROMACS 3.0: a Package for Molecular Simulation and Trajectory Analysis. *J. Mol. Mod.* **2001,** *7*, 306-317.
14. Hünenberger, P. H. In *Advanced Computer Simulation: Approaches for Soft Matter Sciences I*, Holm, C.; Kremer, K., Eds. Springer Berlin Heidelberg, 2005; pp 105-149.
15. McQuarrie, D. A. *Statistical Mechanics*. University Science Books: Sausalito, USA, 2000.